

Evaluation of Local Climate Zone Model in Monitoring Land Use Changes with Emphasis on Physical Growth (Study Area: Tehran)

Seyed Aghil Ebrahimi Kahangi^a, Seyed Ali Almodaresi^{b*}, Farhad Hamzeh^c

^aPh.D. Student in Geography and Urban Planning, Department of Geography, Central Tehran Branch, Islamic Azad University, Tehran, Iran

^bProfessor, Geomorphology, Yazd Branch, Islamic Azad University, Yazd, Iran

^cAssistant Professor, Department of Geography, Central Tehran Branch, Islamic Azad University, Tehran, Iran

Received 7 July 2021; Revised 21 June 2021; Accepted 1 August 2021

Abstract

Land use change and land cover are considered as one of the important and effective factors on global environmental change, so understanding and predicting the causes, processes and consequences of land use change has become a major challenge on the planet. Today, remote sensing technology and GIS are used effectively to identify and quantify land use change and its effects on the environment. The physical development of cities and the expansion of its dimensions is one of the important factors in urban land change that has many environmental, economic and social consequences. In the past few decades, the city of Tehran has faced numerous urban growth and development and surrounding towns, which has caused extensive changes in the urban lands of Tehran and surrounding areas. In this study, the trend of land use changes in Tehran in the past few decades has been studied. In the present study, using Landsat 8 satellite images, the change and transformation of lands in Tehran from 2013 to 2020 was monitored. Images were pre-processed and classified according to the LCZ model in 17 classes. Then, they were classified in SEGA GIS software and analysed by image difference and post-classification methods. The results of image processing and classification show that urban lands are constantly growing and barren lands are increasing on a very small and slow scale. Also, land with dense vegetation has decreased from 2013 to 2020, which in itself can cause serious damage to urban planning for city managers.

Keywords: Land Use, LCZ Model, Physical Development, Remote Sensing

1. Introduction

Land use and land cover as one of the important and effective factors on global environmental change. Land use change affects a wide range of environmental and natural resource characteristics such as water quality, terrestrial and air resources, processes and functions of ecosystems and climate systems (Ahmad, 2014). Therefore, timely and accurate detection of such changes is the basis for a better understanding of the relationships and interactions between humans and natural phenomena, and thus provides better

* Corresponding author Tel: +98.9131526455
Email address: almodaresi@yahoo.com.

management and better use of natural resources (Rostaie et al., 2014). The physical growth of cities may have several environmental, economic and social consequences, so that the physical development of cities due to the sharp increase in population and related activities causes a wide change in land use around cities (Chadchan & Shankar, 2012). Land use change has generally caused many problems such as destruction of natural areas (forests and pastures), destruction of agricultural land, water pollution, soil erosion, increase floods, decrease environmental quality, reduced ecological capacity to produce natural resources, increased land prices and reduced forest and agricultural lands (Akbari et al., 2016). One of the most important issues in land management and sustainable development is recognizing land cover or use and the process of their change. In fact, one of the main preconditions for optimal land use is knowledge of land use patterns and knowledge of changes in each use over time, which can be predicted in the future by knowing the trend of change over time. Urbanization is an important component in the transformation of the world's lands (Samadzadegan et al., 2012). Despite the small percentage of urban land in the world, irregular urban development may lead to widespread changes in the environmental conditions of other land uses. Physical development of cities is a dynamic and continuous process during which the physical boundaries of the city and their physical spaces increase in vertical and horizontal directions in terms of quantity and quality (Sahebjalal & Dashtekian 2013). Urban development is moving towards the outer regions and causing changes in the use of the surrounding lands. Land use change includes changing the type of land uses and changing the distribution and spatial patterns of activities and land uses. Land use changes in case of incompatibility and lack of management may have several negative effects on the quality of resources and soil, species and the status of urban and rural residents (Xian & Crane, 2006). Over the past three decades, due to periodic repetition, spectral and radiometric diversity, integrated vision and digital format suitable for computer processing, remote sensing data is a very suitable data source for various applications, including the preparation of land cover maps. One of the special applications of distance monitoring is environmental monitoring or detection of changes. In the past, environmental monitoring was based on field methods and conventional large-scale photography (Tekle, 2001). Obviously, this method is effective for small and accessible environments and the resources that are located in desert and hard-to-reach areas are not recognizable in this method, while the field method requires significant costs and time. Satellite data is able to accurately and partially detect environmental changes, especially for remote locations, as well as a wide range, and in addition to saving time and study costs (Sardashti et al., 2010).

Sofianian et al. (2009) studied land use changes for the city of Isfahan between 1987 and 1998. The data used in this study were Landsat satellite TM sensor data. In order to detect the changes, the vector analysis method of changes was applied to the images. The results showed that vector analysis of changes is a suitable method for detecting and describing radiometric changes in the time series of multispectral satellite data. The location of the change maps also showed that during the mentioned years, the city has been further south and southeast (Eshaghi et al., 2016).

Using remote sensing and GIS data, Sain and Khanduri (2013) detected land use changes in Punjab, India between 1991 and 2006. The data used in this study were TM, ETM sensor data from Landsat satellite and IRS (-Chadchan & Shankar, 2012). The method of detecting changes was performed after classifying satellite images.

The desired land use areas were obtained and compared with each other. These researchers consider remote sensing and GIS as an efficient and optimal way to generate spatial information and land use planning. Today, remote sensing and GIS technology are among the top and most efficient technologies in the study of environmental change. These techniques are known as primary data sources for studies of land use change and land cover change as well as resource management in recent decades, which has had a significant impact on land management and urban planning.

Houet and Pigeon (2011) used the UCZ scheme to classify the city level in Toulouse and to stimulate related weather conditions based on in situ observations and remote sensing data (Birhane et al., 2019). Emmanuel and Krueger (2013) applied the LCZ in the densely populated city of Glasgow and examined the impact of urbanization on local climate change using 50-year historical data.

Middle et al. (2014) used the ENVI-met model to simulate the local thermal environment in Phoenix and

proposed neighborhood design schemes following the LCZ classification system. The application of LCZ in land surface classification for climate and planning purposes is discussed in the above studies. Most cities, however, are largely adapted by low- and middle-rise buildings, with restrictions on high-end sample sites. Further testing and applications of LCZ are necessary in high-density cities (Garedew et al., 2009).

2. Methods and Materials

2.1. Study Area

The city of Tehran is located at 51 degrees and 6 minutes to 51 degrees and 38 minutes east longitude and 35 degrees and 34 minutes to 35 degrees and 51 minutes north latitude. Its height from the open water level varies between 1800 meters in the north to 1200 meters in the center and 1050 meters in the south. Tehran is located between the Alborz Mountains and the northern edge of the central desert of Iran in a relatively flat plain. Its settlement area leads from the south and southwest to Shahriar and Varamin plains. In the north and east, with the natural limit of the geographical space of Tehran in the mountains and plains, it is determined by two rivers, Karaj in the west and Jajroud in the east, which join near the salt desert in the southeast of Tehran.

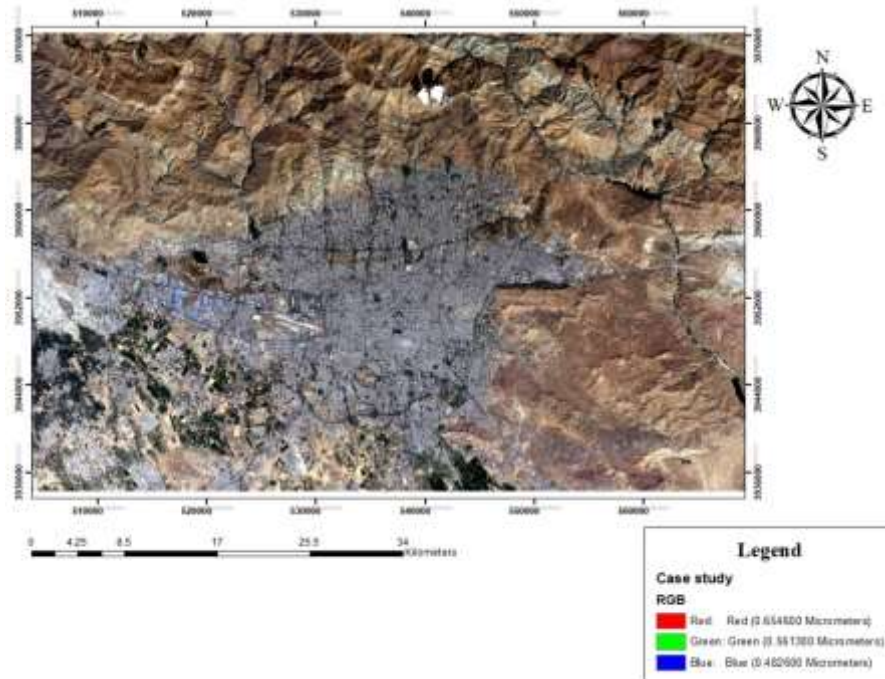


Figure 1. Study area

2.2. Data Used

In this research, Landsat 8 satellite sensor images were used on 10/18/2013 and 9/19/2020. These images are ground reference and are located in the UTM image system in the northern 39th district. The images are available for free on the US Geological Survey at <http://www.usgs.gov>. The images used in this research are all radiometric corrections for all bands and then atmospheric correction for

multi spectral and thermal bands separately. Due to the importance of geometric correction accuracy on the accuracy of change detection results due to pixel-by-pixel comparison of satellite images with each other, these images must be perfectly geometrically compatible with each other. Before processing and comparing these images, geometric correction was performed on them. Due to the reference ground of the mentioned images, from type of geometric corrections, image to image recording was performed.

Table 1. Specifications of the data used

| year | Institution ID LANDSAT | Imaging date |
|------|--|--------------|
| 2013 | LC08_L1TP_164035_20131018_20180526_01_T1_B1 | 2013/10/18 |
| | LC08_L1TP_164035_20131018_20180526_01_T1_B2 | 2013/10/18 |
| | LC08_L1TP_164035_20131018_20180526_01_T1_B3 | 2013/10/18 |
| | LC08_L1TP_164035_20131018_20180526_01_T1_B4 | 2013/10/18 |
| | LC08_L1TP_164035_20131018_20180526_01_T1_B5 | 2013/10/18 |
| | LC08_L1TP_164035_20131018_20180526_01_T1_B6 | 2013/10/18 |
| | LC08_L1TP_164035_20131018_20180526_01_T1_B7 | 2013/10/18 |
| | LC08_L1TP_164035_20131018_20180526_01_T1_B10 | 2013/10/18 |
| | LC08_L1TP_164035_20131018_20180526_01_T1_B11 | 2013/10/18 |
| 2020 | LC08_L1TP_164035_20200919_20201006_01_T1_B1 | 2020/09/19 |
| | LC08_L1TP_164035_20200919_20201006_01_T1_B2 | 2020/09/19 |
| | LC08_L1TP_164035_20200919_20201006_01_T1_B3 | 2020/09/19 |
| | LC08_L1TP_164035_20200919_20201006_01_T1_B4 | 2020/09/19 |
| | LC08_L1TP_164035_20200919_20201006_01_T1_B5 | 2020/09/19 |
| | LC08_L1TP_164035_20200919_20201006_01_T1_B6 | 2020/09/19 |
| | LC08_L1TP_164035_20200919_20201006_01_T1_B7 | 2020/09/19 |
| | LC08_L1TP_164035_20200919_20201006_01_T1_B10 | 2020/09/19 |
| | LC08_L1TP_164035_20200919_20201006_01_T1_B11 | 2020/09/19 |

2.3. LCZ Model

The UCZ scheme is the most universal classification among the above classification systems, but focuses more on modern and developed urban scenarios. With the expansion of UCZ classification work, the LCZ classification system was introduced by Stuart and Oke (2012) to standardize climate observations and facilitate global communication in climate studies. Seventeen major local climatic zones have been identified according to known building forms and types of land cover. Mapping methods have been successfully integrated into the LCZ classification system, which documents and reports spatial information intuitively (Belay and Mengistu 2019; Zhang et al., 2016).

Many cities, such as Nancy, Toulouse, Bilbao, Glasgow, Uppsala, Nagano, and Vancouver, have applied the LCZ classification system to classify land surface characteristics and standardize site selection for climate greenhouses (Kandissounon et al., 2018; Kayet and Pathak 2019; Akpoti et al.,

2016).

2.4. LCZ Mapping Methods

There are basically three LCZ classification methods according to data sources and analytical methods: manual sampling, remote sensing and GIS. Because manual sampling is time consuming and may lead to biased results by different operators, it is not usually applied in city-wide LCZ mapping. Remote Sensing relies on object-based image analysis or pixel-based classification techniques to develop LCZ classification maps from satellite imagery (Arsiso et al., 2018). Pixel-based monitoring method is integrated into the Global Urban Database and Portal Access Tool (WUDAPT) (Yalew et al., 2016). This provides a fast and inexpensive way to classify LCZs based on NASA-supported Landsat remote sensing images (Sobrino et al., 2014).

The GIS method uses more time than the remote sensing method or the manual sampling method, which requires a comprehensive set of planning data. Depending on the data structure, there are two types of GIS methods: Vector method and raster-based method. The vector method has the advantage of creating a cover for objects, because it can follow the exact boundaries of the elements of the ground cover. In comparison, the checkerboard method is more consistent at the geographic scale and more powerful in statistical analysis for its integrated checkerboard networks (Shang and Chisholm 2014; Raj and Vijayan, 2012; Moriasi et al., 2007; Hataminejad et al., 2017). Previous LCZ studies have generally used the vector method in mapping local climatic zones (LCZ).

The LCZ classification scheme divides the landscape into 17 classes, each with a different surface structure, land cover, and human-induced heat dissipation characteristics (hereinafter referred to as "physical characteristics") that affect local temperature. LCZ maps have become an important source of data for studies in urban climatology and urban planning. In a more general context, the LCZ classification scheme has also been proposed as a standard framework for mapping the urban form on a global scale, as it can provide information about the basic physical characteristics of each urban area. For this purpose, we show the 17 classification classes of this model in Figure 2 (Gomez et al., 2016; Mahendra et al., 2015).








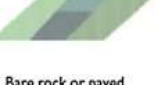


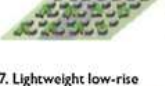

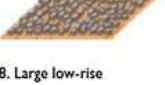




| Built types | Definition | Land cover types | Definition |
|--|--|--|--|
| 1. Compact high-rise  | Dense mix of tall buildings to tens of stories. Few or no trees. Land cover mostly paved. Concrete, steel, stone, and glass construction materials. | A. Dense trees  | Heavily wooded landscape of deciduous and/or evergreen trees. Land cover mostly pervious (low plants). Zone function is natural forest, tree cultivation, or urban park. |
| 2. Compact mid-rise  | Dense mix of midrise buildings (3–9 stories). Few or no trees. Land cover mostly paved. Stone, brick, tile, and concrete construction materials. | B. Scattered trees  | Lightly wooded landscape of deciduous and/or evergreen trees. Land cover mostly pervious (low plants). Zone function is natural forest, tree cultivation, or urban park. |
| 3. Compact low-rise  | Dense mix of low-rise buildings (1–3 stories). Few or no trees. Land cover mostly paved. Stone, brick, tile, and concrete construction materials. | C. Bush, scrub  | Open arrangement of bushes, shrubs, and short, woody trees. Land cover mostly pervious (bare soil or sand). Zone function is natural scrubland or agriculture. |
| 4. Open high-rise  | Open arrangement of tall buildings to tens of stories. Abundance of pervious land cover (low plants, scattered trees). Concrete, steel, stone, and glass construction materials. | D. Low plants  | Featureless landscape of grass or herbaceous plants/crops. Few or no trees. Zone function is natural grassland, agriculture, or urban park. |
| 5. Open mid-rise  | Open arrangement of midrise buildings (3–9 stories). Abundance of pervious land cover (low plants, scattered trees). Concrete, steel, stone, and glass construction materials. | E. Bare rock or paved  | Featureless landscape of rock or paved cover. Few or no trees or plants. Zone function is natural desert (rock) or urban transportation. |
| 6. Open low-rise  | Open arrangement of low-rise buildings (1–3 stories). Abundance of pervious land cover (low plants, scattered trees). Wood, brick, stone, tile, and concrete construction materials. | F. Bare soil or sand  | Featureless landscape of soil or sand cover. Few or no trees or plants. Zone function is natural desert or agriculture. |
| 7. Lightweight low-rise  | Dense mix of single-story buildings. Few or no trees. Land cover mostly hard-packed. Lightweight construction materials (e.g., wood, thatch, corrugated metal). | G. Water  | Large, open water bodies such as seas and lakes, or small bodies such as rivers, reservoirs, and lagoons. |
| 8. Large low-rise  | Open arrangement of large low-rise buildings (1–3 stories). Few or no trees. Land cover mostly paved. Steel, concrete, metal, and stone construction materials. | VARIABLE LAND COVER PROPERTIES | |
| 9. Sparsely built  | Sparse arrangement of small or medium-sized buildings in a natural setting. Abundance of pervious land cover (low plants, scattered trees). | b. bare trees | Leafless deciduous trees (e.g., winter). Increased sky view factor. Reduced albedo. |
| 10. Heavy industry  | Low-rise and midrise industrial structures (towers, tanks, stacks). Few or no trees. Land cover mostly paved or hard-packed. Metal, steel, and concrete construction materials. | s. snow cover | Snow cover >10 cm in depth. Low admittance. High albedo. |
| | | d. dry ground | Parched soil. Low admittance. Large Bowen ratio. Increased albedo. |
| | | w. wet ground | Waterlogged soil. High admittance. Small Bowen ratio. Reduced albedo. |

Figure 2. LCZ model classification classes

3. Results and Discussion

WUDAPT represents a standard workflow for producing LCZ maps that show different types of built-in and natural land cover. This consists of three main steps: First, Landsat image pre-processing: Landsat images were converted into an image to cover the study area. Then, this image was sampled from a resolution of 30 meters to 100 meters and cut to fit the area. Second, the selection of training examples: Polygons, training examples for all types of LCZs available from Google Earth based on local knowledge are digitized, as shown in Figure 3.

In this article, each type of LCZ includes about 20 training samples that have been collected from East Tehran - West Tehran - South Tehran - Central Tehran and North Tehran. Third, LCZ classification by

random forest classifier: Landsat pre-processed images and selected training samples were used to teach random forest classification (Ward et al., 2000). Using the LCZ classification tool in GIS SAGA software. In Figures 4 and 5, you can see the map produced by this model for 2013 and 2020.

The stochastic classifier acts as the ideal compromise between the accuracy obtained and the computational performance among the previously tested classifiers. In addition, the classifier is non-parametric and this is necessary because each LCZ can have completely different patterns or appearances in a city. Also, random forest without the need for additional test data provides error estimation without bias (Muzein 2006; Garedew et al., 2009). Hence it as the final configuration for LCZ classification. Each tree in the classification is constructed using a sample in which about one-third of the observations are omitted. Once all the trees have been created, the resulting class for a set of inputs is based on a majority vote. Finally, manual corrections were made to the historic LCZ maps, which are based on the assumption that the types built do not go back to the natural land cover types. According to the 2013 LCZ map as a reference, the areas that are known as the built type, and we have done the same process for 2020.

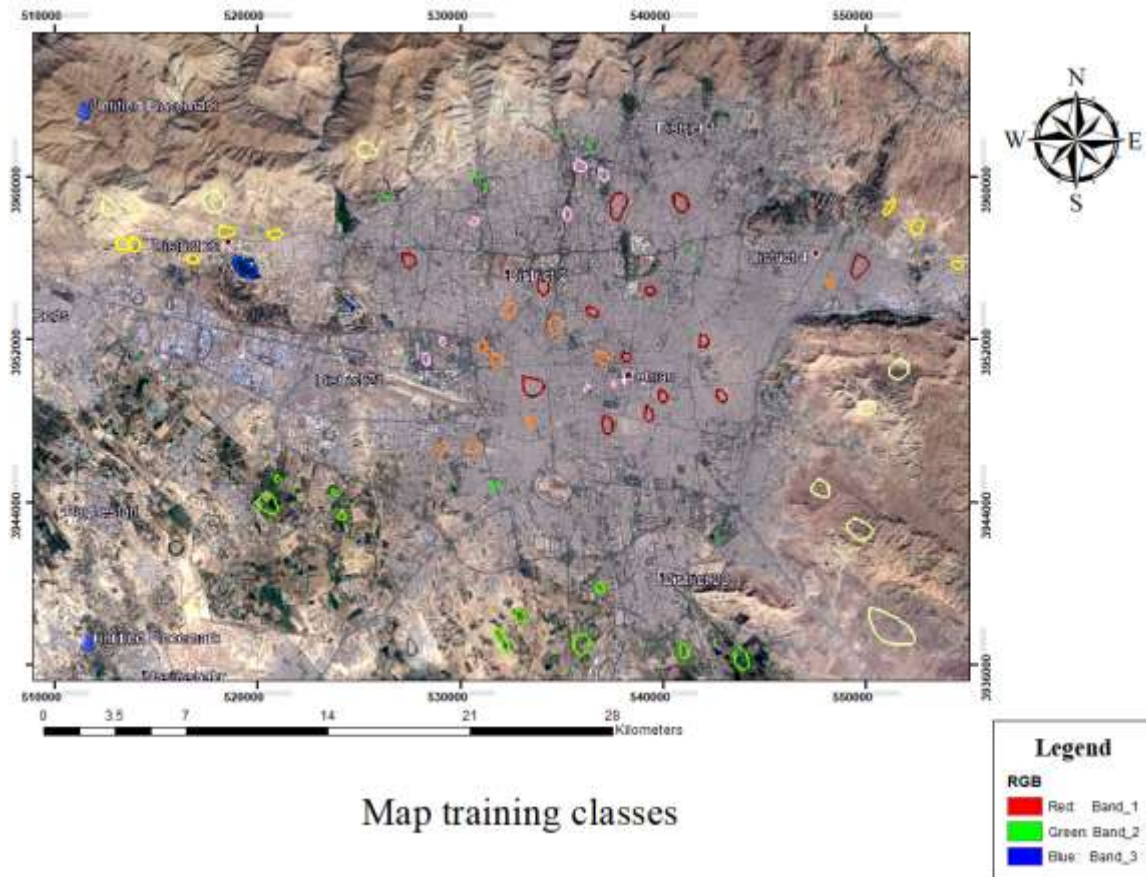


Figure 3. 17 story training sample map of LCZ model

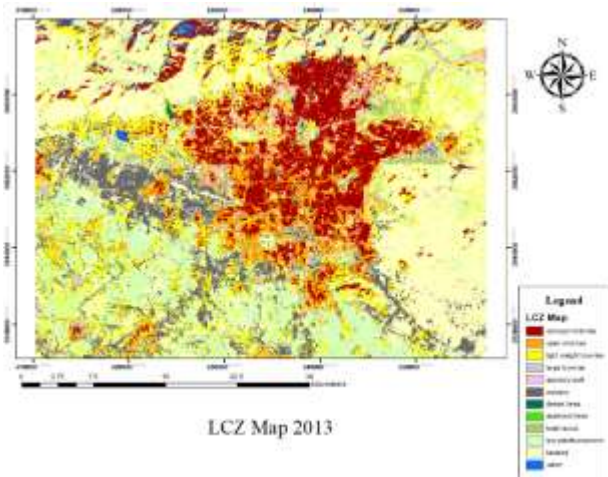


Figure 4. Classified map of 2013

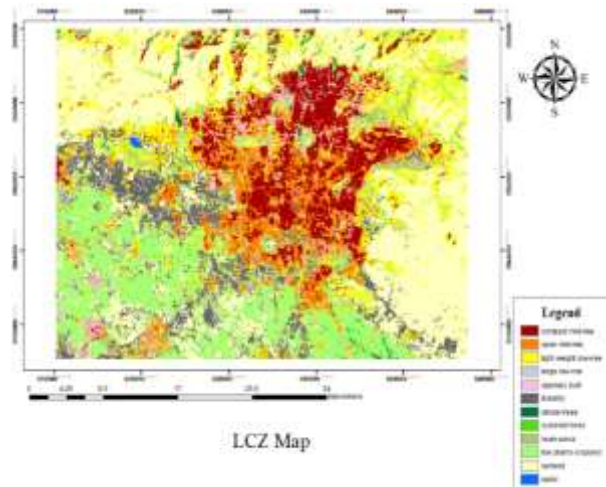


Figure 5. Classified map of 2020

After analyzing the classes classified in the maps used, the amount of each class is prepared as a bar chart for 2013 and 2020 for the LCZ model, which we show in Figures 6 and 7.

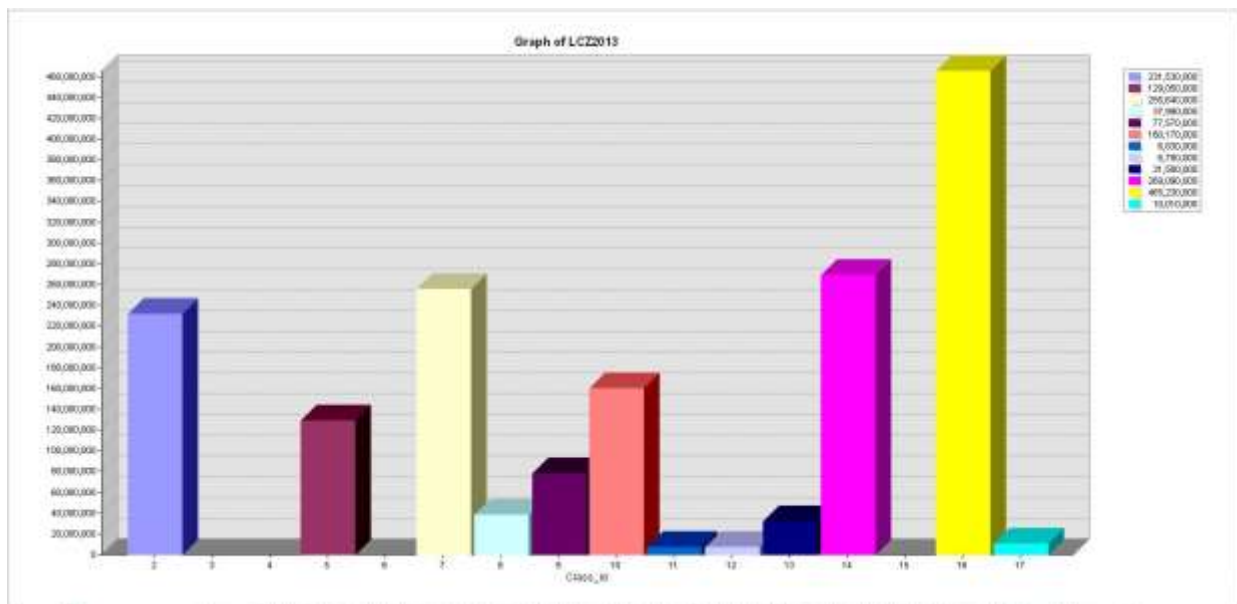


Figure 6. Graph of area in 2013 in square meters

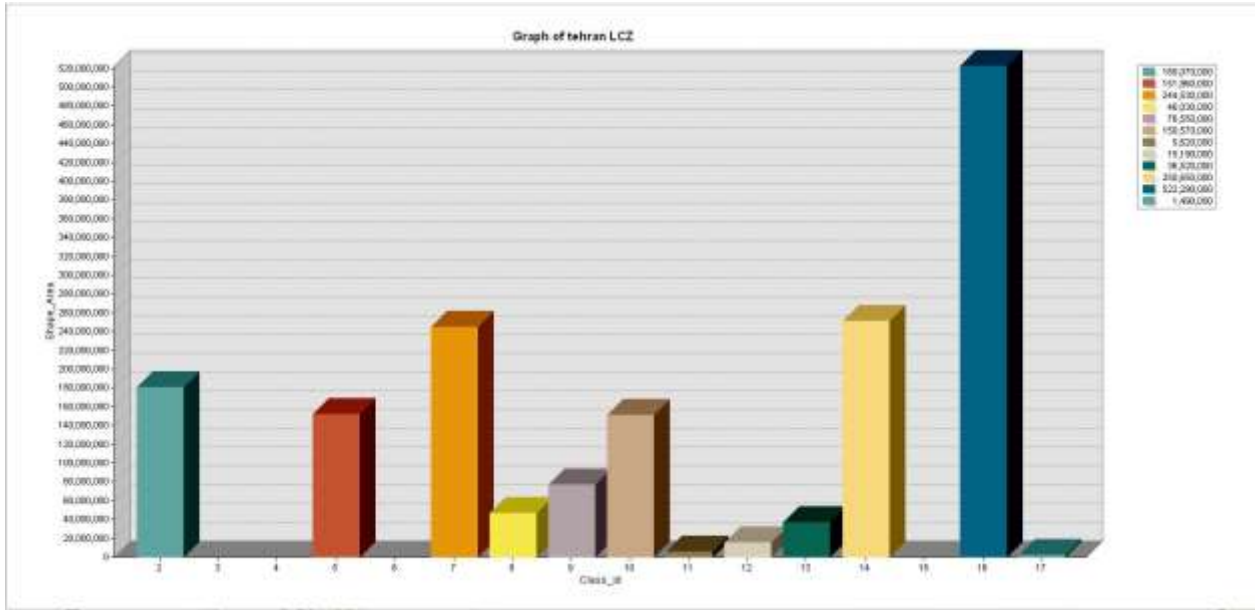


Figure 7. Graph of area in 2020 in square meters

3.1. Assessing the Accuracy of Classification

No classification can be cited until its accuracy has been assessed, except when pixels are sampled as a pattern for spectral or information classes. Assessing the spectral reflectance of classes and their separability can also be done simultaneously (Eshaghi et al., 2016).

Therefore, to ensure the accuracy of the classification, the accuracy of the classification is evaluated (Jafari, 2009). One of the most common methods of expressing classification accuracy is to prepare a classification error matrix (Hajabasi et al., 2001; Zhou et al., 2004). The error matrix compares the relationship between known reference data (terrestrial facts) and the related results of an automated classification by category.

In an error matrix, the parameters of overall accuracy 3, manufacturer accuracy 4, application accuracy and kappa coefficient are calculated. These parameters are the most common parameters for estimating accuracy (Sharifikia et al., 2010). As a result, the error matrix and the mentioned parameters were calculated with the samples taken from the field visits and Google Earth software.

It should be noted that due to the number of 17 classification classes, the error rate in this method is lower than other classification methods such as maximum similarity, minimum distance, iso Data. Therefore, because our study area is the city of Tehran and a large amount of data from each class is defined in it, the accuracy of this method is lower than the usual methods, which can be seen in Tables 2 and 3 (Rabie et al., 2005).

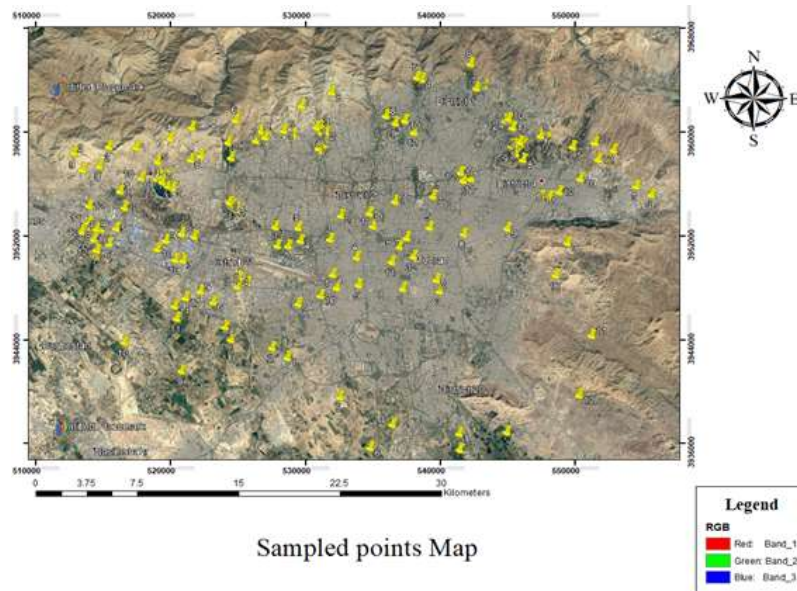


Figure 8. Sampled points for accuracy evaluation

Table 2. Assessing the accuracy of the 2013 user map

| Overall Accuracy = (89/141) 63.1206% | | | | |
|--------------------------------------|-------------------------|------------------------|------------------------|-----------------------|
| Kappa Coefficient = 0.5974 | | | | |
| Class | Prod. Acc. (Percent) | User Acc. (Percent) | Prod. Acc. (Pixels) | User Acc. (Pixels) |
| compact mid-r | 91.67 | 52.38 | 11/12 | 11/21 |
| open mid-rise | 50.00 | 46.15 | 6/12 | 6/13 |
| light weight | 58.33 | 58.33 | 7/12 | 7/12 |
| large low-rise | 16.67 | 50.00 | 2/12 | 2/4 |
| sparsely built | 50.00 | 50.00 | 6/12 | 6/12 |
| industry | 66.67 | 50.00 | 8/12 | 8/16 |
| dense trees | 66.67 | 80.00 | 8/12 | 8/10 |
| scattered tree | 25.00 | 75.00 | 3/12 | 3/4 |
| bush-scarab | 66.67 | 72.73 | 8/12 | 8/11 |
| cropland | 83.33 | 66.67 | 10/12 | 10/15 |
| Breland | 100.00 | 80.00 | 12/12 | 12/15 |
| water | 88.89 | 100.00 | 8/9 | 8/8 |

Table 3. Assessing the accuracy of the 2020 user map

| Overall Accuracy = (91/141) 64.5390% | | | | |
|--------------------------------------|-------------------------|------------------------|------------------------|-----------------------|
| Kappa Coefficient = 0.6130 | | | | |
| Class | Prod. Acc. (Percent) | User Acc. (Percent) | Prod. Acc. (Pixels) | User Acc. (Pixels) |
| compact mid-r | 91.67 | 52.38 | 11/12 | 11/21 |
| open mid-rise | 33.33 | 28.57 | 4/12 | 4/14 |
| light weight | 58.33 | 70.00 | 7/12 | 7/10 |
| large low-rise | 25.00 | 75.00 | 3/12 | 3/4 |
| sparsely built | 50.00 | 66.67 | 6/12 | 6/9 |
| industry | 91.67 | 57.89 | 11/12 | 11/19 |
| dense trees | 50.00 | 60.00 | 6/12 | 6/10 |
| scattered tree | 25.00 | 37.50 | 3/12 | 3/8 |
| bush-scrub | 66.67 | 88.89 | 8/12 | 8/9 |
| low plants | 91.67 | 68.75 | 11/12 | 11/16 |
| Breland | 100.00 | 100.00 | 12/12 | 12/12 |
| water | 100.00 | 100.00 | 9/9 | 9/9 |

4. Conclusion

The results of overall accuracy and kappa coefficient obtained in Landsat 8 images to investigate the amount of changes in the Tehran region using the LCZ method showed that satellite images are capable of detecting changes. In this study, results with relatively high accuracy according to the method performed compared to similar research have been obtained (Sanjari 2013; Ebrahimi et al., 2016). Due to the use of Google Earth software images in the preparation of educational points, the high level of educational points and accuracy in selecting educational points. Over time, land cover patterns and consequently land use change fundamentally and the human factor can play the most important role in this process (Bewket, 2002). One of the factors affecting land use is population growth. Urban development is closely related to the rate of urban population growth and in this regard, the natural increase of the city, the rate of net migration to the city, the transfer of population construction of non-urban communities to the city and the construction of urban population are the main factors (Katpatal et al., 2008; Schneider, 2012).

Migration, as one of the political, economic and social disabilities that has a major impact on the creation of new socio-economic structures, has a major role in the development of the city and its change of use. As a result of the results, it can be concluded that urban areas with green space between them in 2020 has a significant growth compared to 2013. Barren lands have increased in 2020 compared to 2013, so we can say that the outskirts of Tehran are increasing. And it can be predicted that in the coming years this wasteland will become residential or other uses. As a result, given that knowledge of land use patterns and its changes over time is a prerequisite for the optimal use of national capital (Qin and Karnieli, 1999). Therefore, the extraction of land use roles can be considered as the most important goal in the management of the urban management base. Currently, the use of remote sensing technology is the best tool for extracting maps related to land uses (Mahendra et al., 2015; Xu et al., 2008).

In natural resource management and environment and urban management, planning for land use, preparing land use maps and recognizing the potential and talent of lands is necessary and is an important source of information for adopting principled policies and developing development plans. Therefore, land use information, as basic information, plays a very important role in the management of natural and urban resources (Xu et al., 2012). But the problem with urban planning, which almost all natural resource planners and policymakers agree on, is that resources are declining and will continue to be exploited

with current methods (Abedine and moghimi, 2011).

References

- Akbari, A., Zangane asadi, M. A., & Taghavi moghadam, A. (2016). Land change monitoring using different methods of Naishabor district statistical education theory. *Spatial planning of space*, 20(6), 35-50.
- Abedini, M., & Moghimi, E. (2012). The role of geomorphological bottlenecks in the physical development of Tabriz metropolis for optimal use. *Geography and environmental planning*, 23(1), Isfahan, 147-166.
- Ahmad, S. (2014). Land use change detection using remote sensing and artificial neural network: Application to Birjand, Iran. *Computational Ecology and Software*, 4, 276.
- Akpoti, K., Antwi, E. O., & Kabo-Bah, A. T. (2016). Impacts of rainfall variability, land use and land cover change on stream flow of the black Volta Basin, West Africa. *Hydrology*, 3(3), 26.
- Arsiso, B. K., Tsidu, G. M., Stoffberg, G. H., & Tadesse, T. (2018). Influence of urbanization-driven land use/cover change on climate: the case of Addis Ababa, Ethiopia. *Physics and Chemistry of the Earth, Parts A/B/C*, 105, 212–223.
- Belay, T., & Mengistu, D. A. (2019). Land use and land cover dynamics and drivers in the Muga watershed, Upper Blue Nile basin, Ethiopia. *Remote Sensing Applications. Society and Environment*, 15, 100249.
- Bewket, W. (2002). Land cover dynamics since the 1950s in Chemoga watershed, Blue Nile basin, Ethiopia. *Mountain Research and Development*, 22(3), 263–269.
- Birhane, E., Ashfare, H., Fenta, A. A., Hishe, H., Gebremedhin, M. A., & Solomon, N. (2019). Land use land cover changes along topographic gradients in Hugumburda national forest priority area, Northern Ethiopia. *Remote Sensing Applications: Society and Environment*, 13, 61-68.
- Chadchan, J., & Shankar, R. (2012). An analysis of urban growth trends in the post-economic reforms period in India. *International Journal of Sustainable Built Environment*, 1(1), 36-49.
- Chandra, S., Sharma, D., & Dubey, S. K. (2018). Linkage of urban expansion and land surface temperature using geospatial techniques for Jaipur City, India. *Arabian Journal of Geosciences*, 11(2), 1-12.
- Ebrahimi, P., Eslah, M., & Salimi koshi, J. (2016). Studying the performance of the Markov chain in estimating the changes in land use and land cover using Landsat satellite imagery. *Science and engineering department*, 10(34), 85-92.
- Eshaghi, M. A., & Shetaie joybari, Sh. (2016). Fire hazard map using backup vector algorithms, stochastic forest and artificial neural network case study: Golestan, National Park, northeast of Iran. *Research and Science Research and Technology Studies*, 23(4), 133-154.
- Krueger, E., & Emmanuel, R. (2013). Accounting for atmospheric stability conditions in urban heat island studies: The case of Glasgow, UK. *Landscape and Urban Planning*, 117, 112-121.
- Garedew, E., Sandewall, M., Söderberg, U., & Campbell, B. M. (2009). Land-use and land-cover dynamics in the central rift valley of Ethiopia. *Environmental Management*, 44(4), 683–694. <https://doi.org/10.1007/s00267-009-9355-z>
- Geremew, A. A. (2013). Assessing the impacts of land use and land cover change on hydrology of watershed: a case study on Gigel-Abbay Watershed, *Lake Tana Basin, Ethiopia* (Doctoral dissertation).
- Gomez, C., White, J. C., & Wulder, M. A. (2016). Optical remotely sensed time series data for land cover classification: A review. *ISPRS Journal of Photogrammetry and Remote Sensing*, 116, 55–72.
- Hatami Nejad, H., Lorestani, A., Ahmadi, S., & Mohammadi, M. (2017). Analysis of the physical expansion pattern of Khorramabad city using Shannon and Holdern entropy models and determining the optimal directions of its expansion using AHP model. *Journal of Human Geography Research*, 49(3), 519-537.
- Hajabsi, M. A., Jalalian, A., Khajedin, J., & Karimzadeh, H. (2002). Case study of the effect of rangeland conversion into agricultural lands on some physical characteristics, fertility and soil fertility index in Borujen. *Agricultural Science and Technology and Natural Resources*, 6(1), 149-160.

- Jafari, M. (2009). *Evaluation and study of land use change trends in Rasht city using remote sensing and geographic information system*. Master Thesis in Natural Resources Engineering, Land Assessment and Planning, Faculty of Environment and Energy, Islamic Azad University, Science and Research Branch, p.171.
- Kandissounon, G. A., Kalra, A., & Ahmad, S. (2018). Integrating system dynamics and remote sensing to estimate future water usage and average surface runoff in Lagos, Nigeria. *Civil Engineering Journal*, 4(2), 378–393.
- Katpatal, Y. B., Kute, A., & Satapathy, D. R. (2008). Surface-and air-temperature studies in relation to land use/land cover of Nagpur urban area using Landsat 5 TM data. *Journal of Urban Planning and Development*, ASCE, 134(3), 110-118.
- Kayet, N., & Pathak, K. (2015). Remote sensing and GIS based land use/land cover change detection mapping in Saranda Forest, Jharkhand, India. *International Research Journal of Earth Sciences*, 3(10), 1–6.
- Mahendra, H., Shivakumar, B., & Praveen, J. (2015). Pixel-based classification of multispectral remotely sensed data using support vector machine classifier. *IJIREEICE*. doi: 10.17148/IJIREEICE [Google Scholar]
- Moriassi, D. N., Arnold, J. G., Van Liew, M. W., Bingner, R. L., Harmel, R. D., & Veith, T. L. (2007). Model evaluation guidelines for systematic quantification of accuracy in watershed simulations. *Transactions of the ASABE*, 50(3), 885–900. <https://doi.org/10.13031/2013.23153> [Crossref], [Web of Science®], [Google Scholar].
- Middel, A., Häb, K., Brazel, A. J., Martin, C. A., & Guhathakurta, S. (2014). Impact of urban form and design on mid-afternoon microclimate in Phoenix Local Climate Zones. *Landscape and urban planning*, 122, 16-28.
- Muzein, B. S. (2006). Remote sensing & GIS for land cover, land use change detection and analysis in the semi-natural ecosystems and agriculture landscapes of the central Ethiopian Rift Valley. *Verlag nicht ermittelbar*.
- Petropoulos, G. P., Griffiths, H. M., & Kalivas, D. P. (2014). Quantifying spatial and temporal vegetation recovery dynamics following a wildfire event in a Mediterranean landscape using EO data and GIS. *Applied Geography*, 50, 120-131.
- Qin, Z., & Karnieli, A. (1999). Progress in the remote sensing of land surface temperature and ground emissivity using NOAA-AVHRR data. *International journal of remote sensing*, 20(12), 2367-2393.
- Raj, A., & Vijayan, N. (2012). Analysis of land use/land cover changes of Kazhakkuttam block based on GIS. In *Green Technologies (ICGT). 2012 International Conference on. IEEE*, 143–146.
- Rabiee, H., Ziaei Firoozabadi, P., & Ali Mohammadi, A. (2005). Discovery and retrieval of land use changes and land cover in Isfahan using remote sensing and geographic information system. *Quarterly Journal of Planning and Spatial Planning, Golestan*, 9(4), 22-75.
- Roustaei, Sh., Ahadnejad Roshti, M., & Farrokhi Soomeh, M. (2014). A study of spatial measurement of urban area with emphasis on land use changes using multi-time satellite images; Case study: Urmia. *Journal of Geography and Planning*, 18(50), 189-206.
- Schneider, A. (2012). Monitoring land cover change in urban and peri-urban areas using dense time stacks of Landsat satellite data and a data mining approach. *Remote Sensing Environment*, 124, 689–704.
- Shang, X., & Chisholm, L. A. (2013). Classification of Australian native forest species using hyperspectral remote sensing and machine-learning classification algorithms. *IEEE Journal of Selected Topics in Applied Earth Observations and Remote Sensing*, 7(6), 2481-2489.
- Sobrino, J. A., & Jiménez-Muñoz, J. C. (2014). Minimum configuration of thermal infrared bands for land surface temperature and emissivity estimation in the context of potential future missions. *Remote Sensing Environment*, 148, 158–167.
- Sardashti, M., Qanavati, A., Zeyaian, P., & Morshedi, J. (2010). Detection of land use changes in Taleghan watershed from 1987-2002 using Landsat satellite imagery and remote sensing. *National Geomatics Conference, Tehran, National Surveying Organization*, 19 and 20 May.
- Sabzqabai, Gh., Raz, S., Dashti, S., & Yousefi Khankhah, Sh. (2014). Study of Land Use Change Using

- Geographic Information System and Remote Sensing Techniques (Case Study: Andimeshk County). *Journal of Geography and Development*, 15(15), 32-45.
- Sahebjalal E, Dashtekian K (2013) Analysis of land use land covers changes using normalized difference vegetation index (NDVI) differencing and classification methods. *African Journal of Agricultural Research* 8:4614–4622.
- Sanjari, S., & Boroumand, N. (2013). Monitoring land use change / land cover in the last three decades using remote sensing technique (Case study: Zarand region of Kerman province). *Journal of Remote Sensing and Geographic Information System in Natural Resources*, 4(1), 91-105.
- Samadzadegan, F., Tabib Mahmoudi, F., & Bigdeli, B. (2012). *Integration of data in remote sensing and concepts and methods*. Publishing Institute, University of Tehran. 312 pages.
- Sharifikia, M., Motamedinia, M., & Shayan, S. (2010). Spatial analysis of geomorphological hazards due to physical development of Mahneshan city. *Journal of Applied Research in Geographical Sciences*, 13(6), 105-126.
- Sofianian, A. (2009). A study on land use change in Isfahan using. *Water and soil science (Journal of science and technology of agriculture and natural resources)*, 13(49), 153-164.
- Tekle, K. (2001). Natural regeneration of degraded hillslopes in Southern Wello, Ethiopia: A study based on permanent plots. *Applied Geography*, 21(3), 275–300.
- Ward, D., Phinn, S. R., & Murray, A. T. (2000). Monitoring growth in rapidly urbanizing areas using remotely sensed data. *The Professional Geographer*, 52(3), 371–386.
- Xian, G., & Crane, M. (2006). An analysis of urban thermal characteristics and associated land cover in Tampa Bay and Las Vegas using Landsat satellite data. *Remote Sensing Environment*, 104(2), 147–156.
- Xu, Y., Qin, Z., Lv, J. (2008). Comparative analysis of urban heat island and associated land cover change based in Suzhou City using Landsat data. *International Workshop on Education Technology and Training & 2008 International Workshop on Geoscience and Remote Sensing*, 316–319. <https://doi.org/10.1109/ETTandGRS.2008.224>
- Xu, Y., Qin, Z., & Shen, Y. (2012). Study on the estimation of near-surface air temperature from MODIS data by statistical methods. *International journal of remote sensing*, 33(24), 7629-7643.
- Yalew, S. G., Mul, M. L., Van Griensven, A., Teferi, E., Priess, J., Schweitzer, C., & Van Der Zaag, P. (2016). Land-use change modelling in the Upper Blue Nile Basin. *Environments*, 3(4), 21.
- Zhang, F., Tiyip, T., Kung, H., Johnson, V. C., Maimaitiyiming, M., Zhou, M., & Wang, J. (2016). Dynamics of land surface temperature (LST) in response to land use and land cover (LULC) changes in the Weigan and Kuqa river oasis, Xinjiang, China. *Arabian Journal of Geosciences*, 9(7), 1-14.
- Zhou, D., Bousquet, O., Lal, T. N., Weston, J., & Schoellkopf, B. (2004). Learning with local and global consistency. In: *Advances in neural information processing systems*, 321–328.